



Cite this: DOI: 10.1039/c5gc01719j

A bilateral electrochemical hydrogen pump reactor for 2-propanol dehydrogenation and phenol hydrogenation

Shiqi Huang,^a Xuemei Wu,^{*a} Wei Chen,^a Tao Wang,^a Yao Wu^a and Gaohong He^{*a,b}

A bilateral electrochemical hydrogen pump reactor is proposed for the first time. In one electrochemical hydrogen pump (EHP) configuration, *in situ* adsorbed hydrogen atoms for phenol hydrogenation at the cathode are donated by the dehydrogenation of 2-propanol instead of a conventional H₂ or H₂O anode feedstock. For the anodic 2-propanol dehydrogenation EHP reactor, by increasing Pt–Ru/C catalyst loading and applying a pulse current operation, the applied potential can be controlled below 0.2 V, which is much lower than the thermodynamic dissociation potential of water (1.23 V). For the cathodic cyclohexanone hydrogenation EHP reactor, the hydrogenation rate reaches 73.9 mmol h⁻¹ g⁻¹_{Pd}, nearly three times of that in aqueous-phase selective hydrogenation reactors. Pd/C and Pt/C catalysts have high catalytic selectivity to cyclohexanone (95.5%) and cyclohexanol (95.4%), respectively. In the bilateral EHP reactor, 2-propanol dehydrogenation and phenol hydrogenation are completed simultaneously, exhibiting a comparable hydrogenation rate, selectivity and conversion to that in the individual EHP reactors. The feasibility of the bilateral EHP reactor provides a novel idea to efficiently integrate multiple reactors into one configuration, which greatly simplifies hydrogen production, storage and transportation, as well as reactor equipment.

Received 26th July 2015,
Accepted 23rd October 2015

DOI: 10.1039/c5gc01719j

www.rsc.org/greenchem

1. Introduction

Biofuels play an important role in offering renewable energy worldwide, which poses the cardinal environmentally friendly energy solution in many fields.^{1,2} Hydrogenation is an essential process for aqueous bio-oil to be transformed into biofuel. Due to the limited solubility of hydrogen in water (merely 1.565 g H₂ per cubic meter water),³ conventional heterogeneous hydrogenation requires an excessive amount of pure hydrogen to be fed into the system at a high pressure and temperature to achieve a desirable hydrogenation rate. It dissipates a great amount of energy.⁴

Recently, an EHP hydrogenation reactor, with the same configuration as a polymer electrolyte membrane fuel cell,^{5,6} has provided an alternative to heterogeneous catalytic hydrogenation, due to its ability to produce dissociated hydrogen *in situ* on a catalyst surface with high efficiency. In an EHP hydrogenation reactor, water or hydrogen is oxidized to generate

protons at an anode under an applied potential,⁷ and the produced protons transfer to a cathode and directly take part in the hydrogenation of biomass derivatives on the cathode catalyst surface. Compared with the harsh conditions in conventional heterogeneous reactors, such as slurry and autoclave reactors, *in situ* dissociated hydrogen in an EHP reactor reduces the resistance of hydrogen transfer to the greatest degree, therefore an EHP hydrogenation reactor exhibits excellent performance at ambient pressure and temperature.^{7–12}

The EHP hydrogenation reactor has attracted intense attention in biomass hydrofining due to its notable advantages. Researchers have investigated related topics with regard to reactants, operation conditions and EHP structures. Among them, hydrogenation of furfural,⁸ acetophenone⁹ and selective reduction of levulinic acid¹⁰ at the cathode are remarkable examples. Acetone, as a model biomass compound, was investigated by Benziger¹¹ and Green⁷ to optimize the reaction conditions and catalysts. They revealed that a current density of 10 mA cm⁻² in the EHP reactor is equivalent to a 100 bar hydrogen partial pressure with regard to providing dissociated hydrogen on the catalyst surface, thereby achieving the biomass hydrogenation target in milder conditions. In our previous work, Chen¹² studied the effects of the hydrophobicity of the diffusion layer on mass transfer resistance of biomass model compounds with different volatilities, highlighting the

^aState Key Laboratory of Fine Chemicals, Research and Development Center of Membrane Science and Technology, Dalian University of Technology, Dalian, 116024, China. E-mail: xuemeiw@dlut.edu.cn; Tel: (+86) 411-8498-6291

^bSchool of Petroleum and Chemical Engineering, Panjin Campus of Dalian University of Technology, Panjin, 124221, China. E-mail: hgaohong@dlut.edu.cn; Tel: (+86) 427-2631916

importance of EHP reactor configurations on hydrogenation behaviour.

However, there are few concerns about the source of hydrogen for the anode of EHP hydrogenation reactors. In most cases, pure hydrogen is used as an anode feedstock to provide protons to the cathode hydrogenation reaction, which is mainly derived from non-renewable coal and natural gas. Consumption of fossil resources also contributes to global warming and soil acidification.^{13,14} To avoid the drawbacks of using hydrogen proton-donators, some pioneering works have attempted water electrolysis. Although proposed as an eco-friendly and renewable solution for EHP reactors, the theoretical electrolysis potential of water is about 1.23 V and the practical potentials are usually over 2.0 V in the literature,¹¹ resulting in energy consumption hundreds of times more than that of hydrogen electrolysis.⁷ Therefore, it is essential to develop a new dehydrogenation technique at the anode to promote applications of EHP hydrogenation reactors on a large scale.

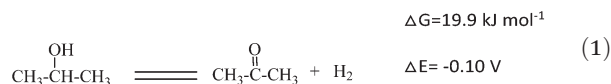
In the literature, dehydrogenation reactions often aim at producing valuable organic chemicals, such as ketones and alkenes, using alcohols and alkanes as dehydrogenation reactants. They usually take place in conventional three-phase reactors and require a high temperature. For instance, Keule¹⁵ and Lambert¹⁶ investigated the dehydrogenation of 2-butanol to generate methyl ethyl ketone and butane. The reaction temperature was over 200 °C, which is the usual temperature used to compensate the reaction kinetics. Dehydrogenation reactions have also been investigated in fuel cells to explore alternative fuels to hydrogen. It was reported that cyclohexane¹⁷ and ethane¹⁸ were dehydrogenated in a proton exchange membrane fuel cell (PEMFC) to produce olefins and aromatics. Alcohols, in particular methanol, were dehydrogenated to serve as a potential hydrogen source for direct alcohol fuel cells (DAFCs).^{19–21} Quite recently, the EHP was explored as a dehydrogenation reactor. Inspiring results have been achieved by Kim²² and Consuegra²³ in that protons could be produced by the dehydrogenation of glycerol and ethylene glycol in an EHP reactor.

In this paper, it is proposed for the first time that EHP is used as a reactor to complete organic dehydrogenation and biomass derivative hydrogenation simultaneously (denoted as a bilateral EHP reactor hereafter). Owing to the unique membrane barrier effect of EHP reactors, dehydrogenation and hydrogenation reactions could run simultaneously at the anode and cathode compartments without interference. This parallel layout is impossible to achieve in conventional electrocatalytic and three phase reactors, where reactants and products of the two reactions have to be mixed together and are mutually affected by inevitable interaction. For instance, in thermal catalytic coupling reactions,^{24–29} the *in situ* hydrogen derived from dehydrogenation could greatly improve hydrogenation efficiency.²⁴ The reaction heat needed for endothermic dehydrogenation could be compensated by the exothermic hydrogenation to some extent.^{26–29} However, product separation and high temperature operation (at least 200 °C) are still required.

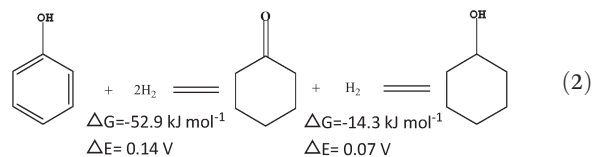
Incorporation of two reactions into one EHP reactor greatly simplifies the reactor equipment. More importantly, in a bilateral EHP reactor, hydrogen is produced by the dehydrogenation of organics instead of water or pure hydrogen, which is promising from an economic aspect in producing valuable products, *i.e.* the dehydrogenation product at the anode as well as the hydrogenation product at the cathode. Organic dehydrogenation reactants usually have lower electrochemical energy barriers than water, which contributes to the reduction of the electrolysis potential and energy consumption.

In this work, 2-propanol and phenol have been investigated as anode and cathode reactants, respectively in a bilateral EHP reactor. Reactions and standard electrode potentials at 25 °C are listed in eqn (1) and (2). At the anode, 2-propanol has a much lower electrolysis potential than that of water. It shows a much higher performance and much lower fuel crossover than methanol in DAFCs.^{30–33} Acetone, as the main product of 2-propanol electro-dehydrogenation,³⁴ is an important organic chemical. In addition, the high solubility of 2-propanol in water poses an incomparable advantage over alkanes, as the water-soluble nature of the reactants is essential to maintain the hydration of the proton exchange membrane. As to the cathode, phenolic compounds are major components of bio-oil with a content percentage of around 7–8 wt%.³⁵ Hydrodeoxygenation of phenolic compounds is an important method used to increase the stability of biofuels. Phenol is the simplest and the most representative compound in the phenolic category. There are two main hydrogenation products of phenol, cyclohexanone and cyclohexanol.^{36,37} Cyclohexanone is an important intermediate for production of nylon 6 and nylon 66.³⁸ Cyclohexanol is the product of further hydrogenation of cyclohexanone, and is a promising component of biofuels. There have been several investigations of the hydrogenation of phenol in the literature. For instance, Güvenatam³⁶ used an acid-Pd/C dual-catalyst for the deep hydrogenation of phenol in autoclave reactors at 200 °C. Liu³⁹ obtained high selectivity and conversion of phenol over a dual supported Pd-Lewis acid catalyst. And Cirtiu³⁷ developed the concept of *in situ* electro-catalytic hydrogenation by exploring the hydrogenation of phenol in an electrochemical dynamic cell. However, few reports can be found on phenol hydrogenated in an EHP reactor.

Anode reaction:



Cathode reaction:



The bilateral EHP reactor runs successfully in this work. At the anode, acetone as well as protons is obtained by the dehydrogenation of 2-propanol. The applied potential for the 2-pro-

panol dehydrogenation EHP reactor is controlled below 0.2 V by increasing Pt–Ru/C catalyst loading and applying a pulse current operation, which is much lower than that of water electrolysis. At the cathode, the cyclohexanone hydrogenation rate in the EHP hydrogenation reactor is nearly three times that in aqueous-phase catalysis by a Pd–PVP catalyst.⁴⁰

2. Experimental

2.1 Materials

The following chemicals were commercially available: acetone ($\text{C}_3\text{H}_5\text{OH}$, 99%), ethanol ($\text{C}_2\text{H}_5\text{OH}$, 99%), 2-propanol ($i\text{-C}_3\text{H}_7\text{OH}$, 99%), *n*-propanol ($n\text{-C}_3\text{H}_7\text{OH}$, 99%), phenol ($\text{C}_6\text{H}_6\text{O}$, 99%), cyclohexanol ($\text{C}_6\text{H}_{10}\text{O}$, 99%), cyclohexanone ($\text{C}_6\text{H}_8\text{O}$, 99%), phosphoric acid (H_3PO_4 , 99%), 20 wt% Pd/C (Premetek Co. Wilmington, DE), 30 wt% Pt–Ru/C (Johnson Matthey Co.), 5 wt% Nafion solution (DuPont Co.), Nafion 117 (DuPont Co.), the gas diffusion layer (GDL25BC, SGL Co.), and the Pt gas diffusion electrode (GDE, 0.5 mg cm^{-2} Pt, Sunrise Power Co.)

2.2 Preparation of MEAs

Pt–Ru and Pd GDEs were home made by spraying catalyst inks (the ratio was 1 : 3 to 2 : 3 parts Nafion/catalysts, lower aliphatic alcohols were used as a dispersant) on commercialized GDL25BC, then drying at 60 °C. MEAs were prepared by hot-pressing the anode and cathode GDEs on either side of Nafion 117 at 140 °C and 5 MPa for 1 min. Two kinds of MEAs with different catalysts, PtRu–Pt, PtRu–Pd (where the first catalyst means the anode catalyst, and the second means the cathode catalyst) were investigated in this work. The physico-chemical characteristics of the electrodes and catalysts of the anode and cathode are listed in Table 1. The electrochemically active surface areas (ESA) were measured by cyclic voltammetry (CV) of CO stripping (Ivium Technologies A08001) according to previous work.⁴¹ Scanning Electron Microscopy (SEM, TM3000) was used to measure the thicknesses of electrodes. Roughness was calculated by dividing the real active areas of the electrode by the geometric area (5.29 cm^2) of the electrode. Charges of hydrogen adsorption were determined by CV of hydrogen adsorption.

Table 1 Physico-chemical characteristics of the electrodes and catalysts

Property		Pt	Pd	Pt–Ru
Electrode	Loading (mg cm^{-2})	0.5	0.5	2.0
	ESA ($\text{m}^2 \text{ g}^{-1}$)	66.4	47.6	32.7
	Roughness	332	238	654
	Thickness of catalyst layer (μm)	8.2	10.6	25.5
	Charge of hydrogen adsorption (C g^{-1})	84.9	79.4	31.5
Catalyst	BET surface ($\text{m}^2 \text{ g}^{-1}$)	192	189	156
	Carbon size (nm)	30	30	20
	Metal size (nm)	2.8 ± 0.3	3.0 ± 0.5	2.6 ± 0.4

2.3 Electrocatalytic dehydrogenation of 2-propanol at the anode

As shown in Fig. 1, the EHP reactor has the same configuration as a PEMFC, with a 5.29 cm^2 effective reaction area and serpentine flow channels for both the anode and cathode. The catalyst loadings are 0.5 mg cm^{-2} to 2.0 mg cm^{-2} Pt–Ru at the anode and 0.5 mg cm^{-2} Pt at the cathode. 30 mL 2-propanol solution was recycled in the anode compartment at flow rate of 10 mL min^{-1} . With a potential applied (GWInSTEK GPD-3303S DC Power Supply) across the cell, 2-propanol was dehydrogenated to acetone and protons. Under galvanostatic conditions, a constant number of protons was transferred across the proton exchange membrane to generate a certain amount of dissociated hydrogen atoms, reduced to H_2 on the cathode catalyst layer.

Electrocatalytic hydrogenation of phenol at the cathode was performed with either pure H_2 or 2-propanol solution as the anode feedstock. For the pure H_2 anode feedstock, 20 sccm H_2 was saturated with water vapour by passing through a humidifier, and then introduced to the anode (anode inlet shown as dotted line in Fig. 1), while 30 mL phenol aqueous solution was hydrogenated at the cathode. 0.5 wt% phosphoric acid was added into the phenol aqueous solution to simulate the acid environment of bio-oil.

In the bilateral EHP reactor, 2-propanol solution replaced hydrogen as the anode feedstock to provide protons. A schematic of the bilateral reactor is shown in Fig. 1. Dehydrogenation of 2-propanol and hydrogenation of phenol were coupled in one EHP reactor driven by an external power supply. 4.0 mg cm^{-2} Pt–Ru anodes and 0.5 mg cm^{-2} Pt or 0.5 mg cm^{-2} Pd cathodes were used in the experiments.

2.4 Analytic methods

The liquid products of the anode and cathode were detected by gas chromatography (FuLi GC-9790II), equipped with an FFAP column ($30 \text{ m} \times 0.32 \text{ mm}$) and a flame ionization detec-

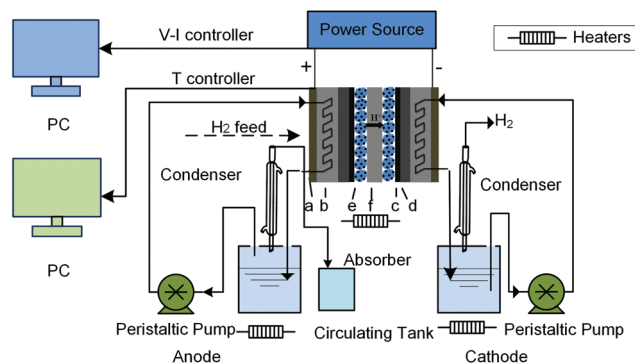


Fig. 1 Schematics of the bilateral EHP reactor (a. current collecting plate; b. serpentine flow channel in graphite blocks; c. microporous layer of GDL (thickness: $235 \mu\text{m}$, air permeability: $1.0 \text{ cm}^3 \text{ cm}^{-2} \text{ s}^{-1}$, crack in microporous layer: $8\text{--}15 \mu\text{m}$); d. macroporous layer of GDL; e. catalyst layer; f. proton exchange membrane Nafion 117 (thickness: $180 \mu\text{m}$, IEC: 0.9 mmol g^{-1} , conductivity: 0.1 S cm^{-1})).

tor. Acetone was determined to be the only product of the anode dehydrogenation reaction, with an *n*-propanol internal standard in the anode aqueous solution. Cyclohexanone and cyclohexanol were detected in the cathode mixture with an *n*-butanol internal standard. The excessive hydrogen produced at the cathode was measured with a soap bubble flowmeter to calculate the total current efficiency. The hydrogenation current efficiency and reaction rate were calculated by eqn (3) and (4), respectively, where mol_{pro} is moles of products detected by GC, n is moles of electrons transferred, F is the Faraday constant ($96485.34 \text{ C mol}^{-1}$), I_{cell} is the current observed in the experiment and Δt is the operational time.

$$\text{Current efficiency} = \frac{\text{mol}_{\text{pro}} n F}{I_{\text{cell}} \Delta t} \quad (3)$$

$$\text{Reaction rate} = \frac{\text{mol}_{\text{pro}}}{\Delta t} \quad (4)$$

3. Results and discussion

3.1. Propanol EHP reactor dehydrogenation at the anode

3.1.1. With Pt/C and Pt-Ru/C catalysts. First, electrocatalytic dehydrogenation of 2-propanol at the anode is investigated in the EHP reactor with purging of hydrogen at the cathode. The catalyst is a crucial parameter that determines the electrolysis potential. Since few references are available on the dehydrogenation of 2-propanol in an EHP reactor, a Pt/C catalyst is selected as the initial choice based on its excellent performance in DAFCs. With a potential applied by DC power across the cell, 2-propanol is dehydrogenated to produce acetone and protons on the anode catalysts. Then acetone is collected at the anode, while protons transfer across the Nafion membrane and reduce to hydrogen at the cathode. As shown in Fig. 2, although stable with reaction time, the overpotential of 2-propanol dehydrogenation on the Pt/C catalyst is much higher than the standard electrode potential of 2-propanol (0.10 V at 25 °C, as shown in eqn (1)), reaching around 0.7 V. In order to reduce the applied potential, Pt-Ru/C, another commonly used catalyst in DAFCs, is tested under the same reaction conditions. With 0.5 mg cm^{-2} Pt-Ru loading, the applied potential is around 0.1 V at the beginning (within 2 min), which is much closer to the standard electrode potential of 2-propanol. It coincides with the research of Lee⁴² that dehydrogenation of 2-propanol initially occurs below 0.2 V on Pt-Ru/C, while it is around 0.65 V on Pt/C catalyst. They suggest that the splitting of the methine C-H is the limiting step of acetone production and the Pt-Ru/C catalyst could reduce the barrier of this elementary step.^{43,44}

With proceeding of the reaction, the applied potential on the Pt-Ru/C catalyst increases dramatically to 1.0 V within 16 min, exhibiting a stage at 0.2–0.42 V, while it only slightly increases on the Pt/C catalyst with instantaneous peaks. The applied potential increase on Pt/C might be caused by production inhibition, that is, the produced acetone takes up

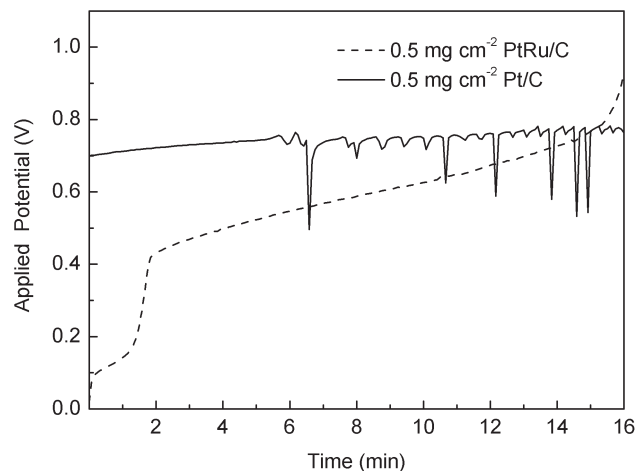


Fig. 2 Applied potential of 2-propanol with different catalysts (reaction conditions: 10 ml min^{-1} 2-propanol, 1 M 2-propanol, 60 °C, 18.9 mA cm^{-2}).

active sites of the catalyst and requires a higher potential to keep the same dehydrogenation rate of 2-propanol.^{31,33} The instantaneous peaks might be caused by CO-type intermediates and Pt-OH formation from water according to one reference.⁴⁵ However, the stepwise potential increase on Pt-Ru/C involves stepwise oxidation of 2-propanol. Previous work⁴² showed that more than one peak was observed in the positive potential scan of the cyclic voltammeter for 2-propanol. 2-Propanol can be oxidized to acetone at a lower applied potential, or be further oxidized into complex products at a higher applied potential. Since Pt-Ru has a higher activity of splitting methine C-H to form acetone, at a constant current density, the produced acetone would be oxidized further before it could desorb from the catalyst surface, leading to a stepwise change of the applied potential.

On the basis of the above analysis, providing sufficient active sites on Pt-Ru/C is the key point in solving the stepwise increase of the applied potential. Two methods are proposed in this work to solve this problem: one is to increase Pt-Ru/C loading to supply more active sites for 2-propanol dehydrogenation; another is pulse current operation to release more acetone from the active sites of the catalyst. Fig. 3 shows the applied potential as a function of catalyst loading or pulse current density.

As shown in Fig. 3(a), with the increase of Pt-Ru loading, the applied potential decreases dramatically and could remain stable around 0.1 V with 2.0 mg cm^{-2} within an operation period of 2 h. In Table 1, it can be seen that the electrode of PtRu (2.0 mg cm^{-2}) has a much larger roughness, providing more active sites for reaction. It is proved that increasing the amount of catalyst active sites could reduce the deep oxidation of 2-propanol, which helps avoid a stepwise increase of the applied potential. Pulse current operation could also relieve the potential jump and help to keep stable the applied potential even with a low catalyst loading. As shown in the inset graph of Fig. 3(b), current density pauses for several

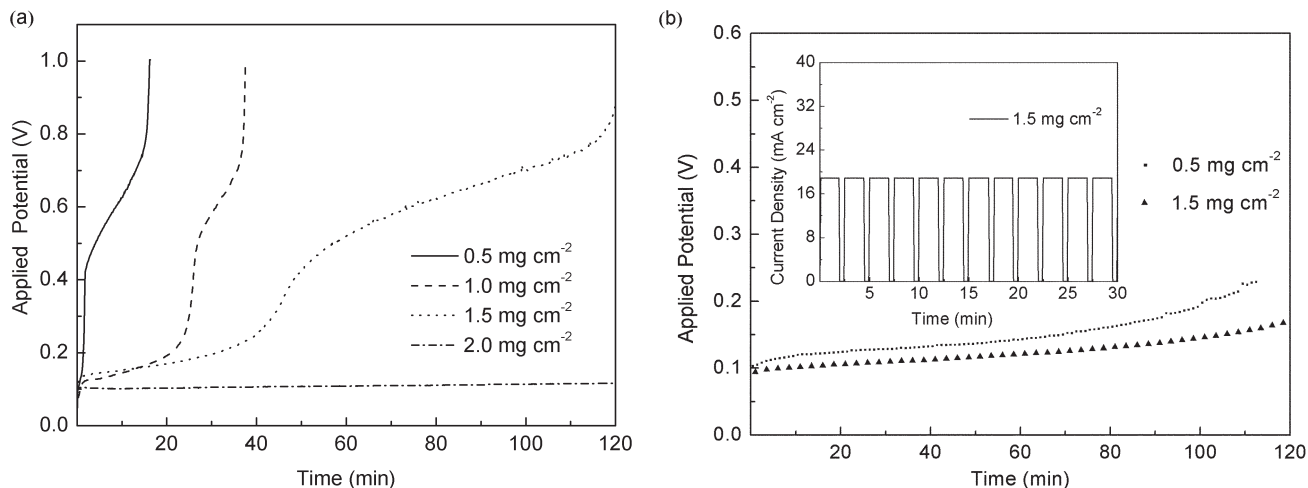


Fig. 3 Applied potential of 2-propanol dehydrogenation as a function of (a) Pt–Ru catalyst loading; (b) pulse current density. Reaction conditions: (a) 10 ml min⁻¹ 2-propanol, 1 M 2-propanol, 60 °C, 18.9 mA cm⁻²; (b) for 0.5 mg cm⁻² Pt–Ru loading, 10 ml min⁻¹ 2-propanol, 1 M 2-propanol, 60 °C, for every cycle, $i = 6.3 \text{ mA cm}^{-2}$ for 30 s, $i = 0 \text{ mA cm}^{-2}$ for 30 s; for 1.5 mg cm⁻² Pt–Ru loading, 10 ml min⁻¹ 2-propanol, 1 M 2-propanol, 60 °C, for every cycle, $i = 18.9 \text{ mA cm}^{-2}$ for 120 s, $i = 0 \text{ mA cm}^{-2}$ for 30 s.

seconds between constant values (pausing 30 s for every 2 min running at 1.5 mg cm⁻², and 30 s for every 30 s running at 0.5 mg cm⁻²). Through this method, the applied potential can remain stable (below 0.2 V for 2 h) with different catalyst loadings of 0.5 mg cm⁻² Pt–Ru and 1.5 mg cm⁻² Pt–Ru, which would otherwise step up to 0.8 V within 15 and 120 min, respectively, at a constant current density (Fig. 3(a)). This result indicates that a stable applied potential could also be achieved by applying a pulse current operation, in which the current density pauses could relieve acetone production inhibition and reset the applied potential at a low level. Pulse current operation controls the applied potential without increasing catalyst loading, and therefore is more economical.

By increasing the loading and applying a pulse current operation, the applied potential for 2-propanol dehydrogenation in an EHP reactor can be controlled below 0.2 V, which is much lower than the thermodynamic dissociation potential of water (1.23 V). The methods proposed in this work also provide guidelines for potential control of stepwise reactions.

3.1.2 Temperature investigation at the anode. Temperature is another main parameter affecting the dehydrogenation rate and applied potential. Based on the maximum operating temperature of the Nafion membrane (80 °C) at atmospheric pressure, the temperature of the EHP reactor was increased from 50 to 80 °C to explore its influence on dehydrogenation performance. Fig. 4 shows the influence of reaction temperature on applied potential, dehydrogenation rate and current efficiency. The applied potential decreases linearly with the increase of temperature, and falls to 0.15 V at 80 °C for 3 h of reaction. This coincides with the theoretical analysis, *i.e.* the electrolysis potential ΔE would decrease due to the decrease of ΔG with the increase of temperature. The current efficiency and dehydrogenation rate are basically constants with the increase of temperature. Under a constant current density of

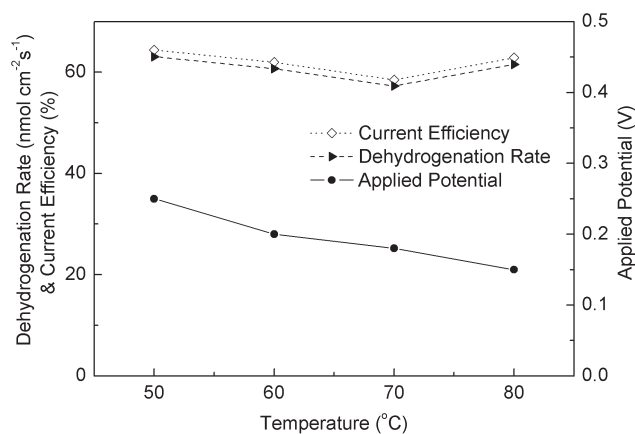


Fig. 4 Rate, current efficiency and applied potential of 2-propanol dehydrogenation as a function of reaction temperature (reaction conditions: 10 ml min⁻¹ 2-propanol, 1 M 2-propanol, 18.9 mA cm⁻², 3 h).

18.9 mA cm⁻², there is the same amount of protons involved in the dehydrogenation reaction, leading to the indistinct variation of the dehydrogenation rate and current efficiency with increasing temperature. According to these results, it is suggested that 80 °C is an optimal temperature for the 2-propanol dehydrogenation EHP reactor.

3.1.3 Available current density by 2-propanol dehydrogenation. One of the advantages of EHP reactors is their ability to provide dissociated hydrogen atoms in an electrochemical way, in which current density is equivalent to the amount of adsorbed hydrogen on the cathode catalyst surface.¹¹

In the novel bilateral reactor, adsorbed hydrogen (or protons) is provided by the dehydrogenation of 2-propanol, and the proton providing capacity is an important part of evaluating the feasibility of the EHP reactor. Experiments were

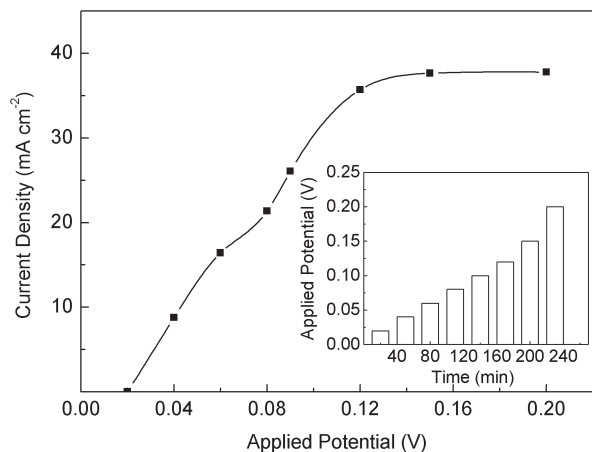


Fig. 5 Available current density of 2-propanol dehydrogenation as a function of applied potential (reaction conditions: 10 ml min⁻¹ 2-propanol, 1 M 2-propanol, 80 °C, 2.0 mg cm⁻² Pt–Ru loading).

conducted in potentiostatic mode at 80 °C, in which steady-state current densities are obtained by applied potential programming from 0.02 to 0.2 V at an interval of 0.02 V, equilibrating for 0.5 h at each applied potential (inset in Fig. 5). As shown in Fig. 5, current density first increases linearly with the increase of applied potential, and then reaches a limiting current at about 0.12 V. The current–potential curve exhibits the same pattern as that with a pure hydrogen anode feedstock, in which the linear increase of current density at a lower applied potential indicates the ohmic resistance domination of the EHP.⁵ The limiting current density (38 mA cm⁻²) is much less than the stoichiometric value (68 mA cm⁻², calculated by Ohm's law at 0.2 V). It is related to product inhibition and 2-propanol transfer limitation, and would become an essential factor at a higher applied potential.

3.2 Phenol EHP electro-catalytic hydrogenation reactor of phenol at the cathode

In this section, phenol is used as a model compound for bio-oil derivatives and its electrocatalytic hydrogenation at the cathode of the EHP reactor is performed with a pure H₂ anode feedstock. The products cyclohexanol and cyclohexanone are valuable materials for organic chemicals and biofuels. Since there are fewer reports on phenol hydrogenation in EHP reactors, different parameters, such as the catalyst, temperature, current density and reaction time are investigated in terms of their influence on phenol hydrogenation.

3.2.1 Temperature investigation at the cathode. Fig. 6 depicts the electrocatalytic hydrogenation of phenol as a function of temperature with different catalysts. Since the hydrogenation products are detected to be cyclohexanol and cyclohexanone by GC, the selectivity of cyclohexanone and cyclohexanol are normalized to 1. Reaction rate, conversion and current efficiency are calculated based on both hydrogenation products, cyclohexanol and cyclohexanone. Applied potentials investigated in all phenol EHP reactors are below 0.05 V. As shown in Fig. 6(a), cyclohexanone is selectively produced on the Pd/C catalyst, achieving a high selectivity of around 80% and remaining stable with increasing temperature. This coincides with the tendency in previous research.^{40,46} Cyclohexanol is the main product on the Pt/C catalyst, reaching a high selectivity of greater than 92.5% at a lower temperature, as shown in Fig. 6(b). Cyclohexanol selectivity on the Pt/C catalyst decreases with the increase of temperature. It might be related to the faster desorption of cyclohexanone from the Pt/C catalyst at elevated temperature, which reduces further hydrogenation of cyclohexanone into cyclohexanol. Reaction rate, current efficiency and conversion go up faster at lower temperatures and increase gradually at higher temperatures on the Pd/C catalyst, while they reach maximum values at around 60 °C on the Pt/C catalyst.

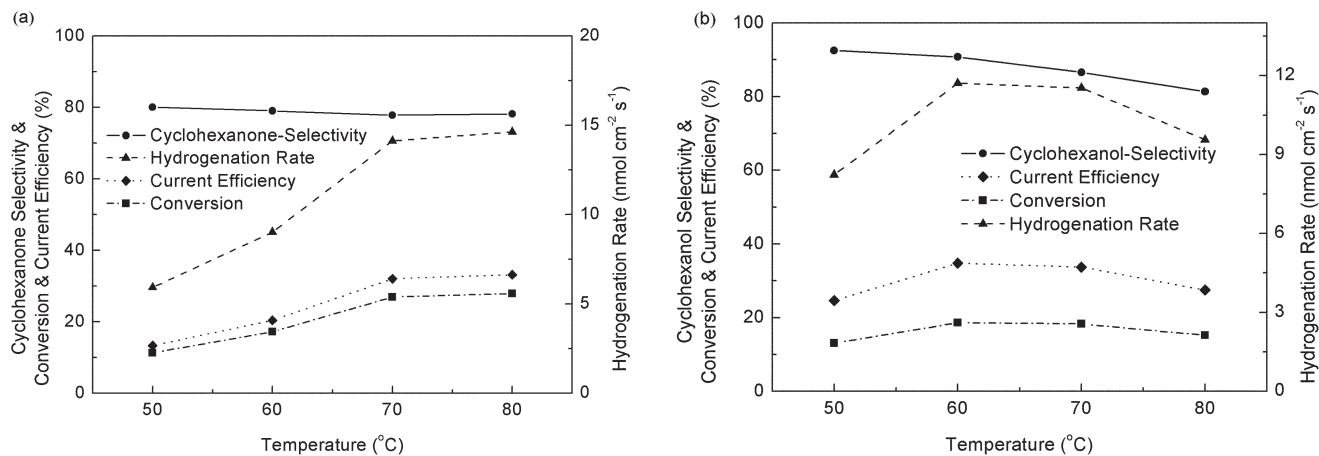


Fig. 6 Cyclohexanone and cyclohexanol selectivity, hydrogenation rate, current efficiency and conversion of phenol as a function of current density catalyzed by (a) Pd/C; and (b) Pt/C (reaction conditions: 20 scfm H₂, 10 ml min⁻¹ phenol, 0.1 M phenol, 18.9 mA cm⁻², catalyst loading: 0.5 mg cm⁻²).

As an exothermic reaction, phenol hydrogenation would reach a maximum reaction rate at a certain optimal reaction temperature instead of increasing with temperature all the time. The results show that the optimal reaction temperature for the product cyclohexanol is around 60 °C, while for the product cyclohexanone it might be higher than 80 °C. The best performance is at 80 °C in the test range.

The EHP phenol hydrogenation reactor in this work exhibits advantages over the reported phenol hydrogenation in the literature. As shown in Fig. 6(a), the rate of the EHP reactor is $11.0 \text{ nmol cm}^{-2} \text{ s}^{-1}$ ($73.9 \text{ mmol h}^{-1} \text{ g}^{-1}_{\text{Pd}}$) based on cyclohexanone at 80 °C under 18.9 mA cm^{-2} (the corresponding total hydrogenation rate is $14.6 \text{ nmol cm}^{-2} \text{ s}^{-1}$ as shown in Fig. 6(a)), which is much higher than that reported in a conventional three-phase reactor with Pd/C at 90 °C and at atmospheric pressure ($9.3 \text{ mmol h}^{-1} \text{ g}^{-1}_{\text{Pd}}$),⁴⁰ as well as the elevated hydrogenation rate in the aqueous phase catalyzed by PVP-Pd ($27.8 \text{ mmol h}^{-1} \text{ g}^{-1}_{\text{Pd}}$). In addition, the results in this paper are based on the overall reaction time, which is much longer than the effective reaction time, *i.e.*, retention time (retention time in this reactor is difficult to precisely calculate). If based on retention time, the hydrogenation rate would be even higher as compared with the conventional reactor.

3.2.2 Current density investigation at the cathode. Since the maximum current density provided by 2-propanol at the anode is 37.8 mA cm^{-2} , current densities ranging from 9.45 mA cm^{-2} to 37.8 mA cm^{-2} are investigated for their effect on phenol hydrogenation. As shown in Fig. 7(a), with increasing current density and catalyzed by Pd/C, the conversion and reaction rate go through a maximum, while current efficiency decreases. As for selectivity, in the range of the tested current density, there is no sign that shows current density influences the selectivity of hydrogenation. At the cathode, there is competition for protons between phenol hydrogenation and hydrogen evolution. With the increase of current density, more protons are transferred to the cathode and promote both

phenol hydrogenation and hydrogen evolution. It is seen from Fig. 7(a) that at higher current densities above 30 mA cm^{-2} , excessive hydrogen evolves on the catalyst surface, and thus blocks the adsorption of phenol and reduces the hydrogenation rate and conversion. The results catalyzed by Pt/C are shown in Fig. 7(b), hydrogenation rate and conversion keep increasing with the increasing current density, which means that the current density is no longer high enough for Pd/C to reach the maximum values. It can be inferred from Fig. 7(b) that cyclohexanol selectivity is more sensitive to current density on the Pt/C catalyst as compared with the Pd/C catalyst, and increases from 53.4% to 95.4% with increasing current density. Higher current density provides more protons for phenol hydrogenation, and it is therefore easier to conduct deep hydrogenation. Taking current efficiency into consideration, it is suggested that 18.9 mA cm^{-2} is enough for Pd/C catalysis to produce cyclohexanone; while the reaction catalyzed by Pt/C needs a higher current density to reach the maximum reaction rate.

3.2.3 Reaction time investigation at the cathode. The effects of reaction time on conversion, current efficiency and reaction rate are shown in Fig. 8. With increasing time, and reducing reaction rate, selectivity and current efficiency, the conversion slowly increases as it reflects the accumulation effect. As the reaction proceeds, the concentrations of cyclohexanone and cyclohexanol increase, which would block active sites for phenol hydrogenation. Fewer catalytic sites cause a reduction of the reaction rate and current efficiency. As for selectivity, a higher concentration of cyclohexanone is produced with increased reaction time and hinders the desorption of cyclohexanone from the catalyst, which favours its further hydrogenation to cyclohexanol. As a result, with the increase of reaction time, cyclohexanone selectivity on the Pd/C catalyst decreases, so 1 h is the optimal reaction time to gain the highest selectivity; while cyclohexanol selectivity on the Pt/C catalyst increases, and the better selectivity is obtained at 3 h.

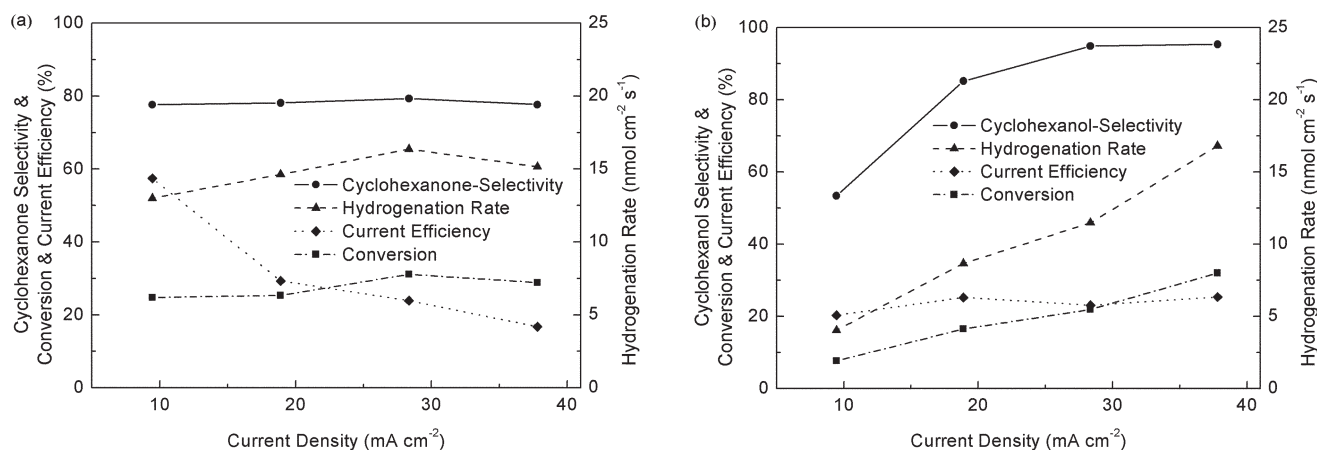


Fig. 7 Cyclohexanone and cyclohexanol selectivity, hydrogenation rate, current efficiency and conversion of phenol as a function of current density catalyzed by (a) Pd/C; and (b) Pt/C; (reaction conditions: 20 sccm H₂, 10 ml min⁻¹ phenol, 0.1 M phenol, 80 °C, 3 h, catalyst loading: 0.5 mg cm⁻²).

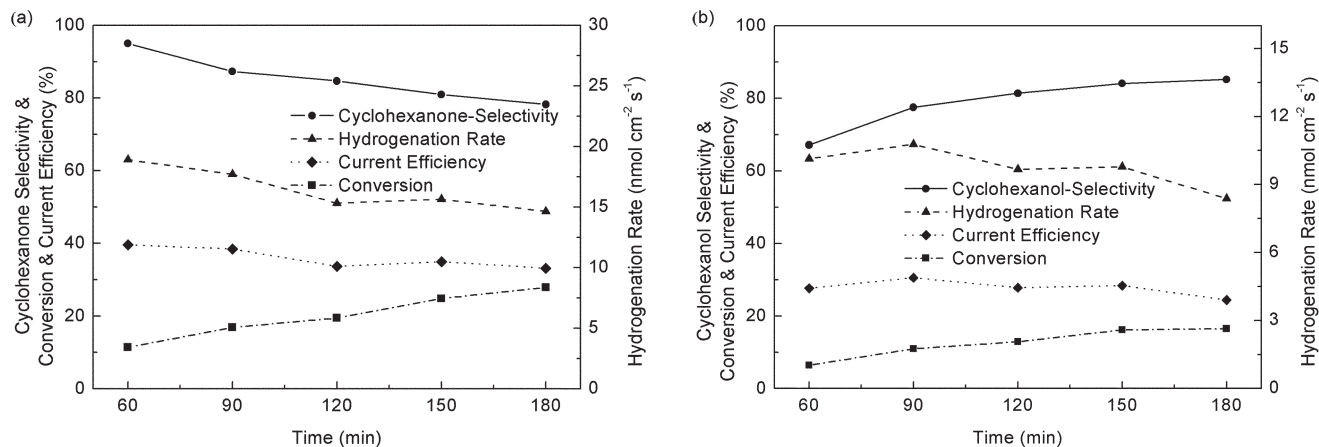


Fig. 8 Cyclohexanone and cyclohexanol selectivity, hydrogenation rate, current efficiency and conversion of phenol as a function of reaction time catalyzed by (a) Pd/C; and (b) Pt/C (reaction conditions: 20 sccm H₂, 10 ml min⁻¹ phenol, 0.1 M phenol, 18.9 mA cm⁻², 80 °C, catalyst loading: 0.5 mg cm⁻²).

3.3 Coupling of 2-propanol dehydrogenation with phenol hydrogenation in an EHP bilateral reactor

The feasibility of combining dehydrogenation and hydrogenation in one EHP reactor is investigated with 2-propanol and phenol as the anode and cathode reactant, respectively. With power supplied, 2-propanol is dehydrogenated at the anode, generating protons for phenol hydrogenation at the cathode. The reaction conditions are selected based on the optimized results of the above experiments, *i.e.*, 80 °C is chosen for the lowest applied potential and the highest cyclohexanone reaction rate; a current density of 18.9 mA cm⁻² is selected for the highest reaction rate based on cyclohexanone. Performance of the EHP bilateral reactor is investigated with a Pt–Ru/C anode catalyst, and Pt/C or Pd/C cathode catalysts, for phenol hydrogenation EHP reactors with a H₂ anode feedstock for 3 h and 1 h.

The results in Fig. 4 show that the anode 2-propanol dehydrogenation rate varies little under a constant current; therefore the phenol hydrogenation performance is the focus for investigating the bilateral reactor. The data in Table 2 show the comparison of the phenol hydrogenation rate, conversion and selectivity in both phenol hydrogenation EHP reactors (H₂ anode feedstock) and bilateral EHP reactors (2-propanol anode feedstock). For the bilateral reactor with PtRu/C-Nafion-Pt/C MEA, the conversion and hydrogenation rate are promoted by about 20%, but cyclohexanol selectivity decreases in contrast with that in the phenol EHP reactor. This indicates a synergistic effect between the anodic and cathodic reactions. As is known, a fully hydrated Nafion membrane has a relatively high hydrogen permeation of about 10⁻⁶ m² s⁻¹, which means that with a hydrogen anode feedstock, hydrogen would permeate from the anode to the cathode and reduce active catalytic sites for phenol hydrogenation. When protons are provided by 2-propanol in the bilateral reactor, much less hydrogen permeation leads to higher performance. As for the PtRu/C-Nafion-Pd/C MEA, cyclohexanone selectivity is comparable, although the conversion and hydrogenation rates of the bilat-

Table 2 Comparison of phenol EHP reactor and bilateral EHP reactor

MEA	Reactor	Conversion (%)	Hydrogenation rate (nmol cm ⁻² s ⁻¹)	Selectivity ^a (%)
PtRu/C-Nafion-Pt/C	Phenol EHP reactor (anode H ₂)	16.5	8.4	85.2
	Bilateral EHP reactor	19.3	10.2	74.3
PtRu/C-Nafion-Pd/C	Phenol EHP reactor (anode H ₂)	11.4	18.0	95.5
	Bilateral EHP reactor	8.0	12.7	93.1

Reaction conditions: 18.9 mA cm⁻², 80 °C; anode: 10 ml min⁻¹ 2-propanol, 1 M 2-propanol, catalyst loading 4.0 mg cm⁻²; cathode: 10 ml min⁻¹ phenol, 0.1 M phenol, catalyst loading 0.5 mg cm⁻², 3 h for PtRu-Nafion-Pt/C; 1 h for PtRu-Nafion-Pd/C. ^aCyclohexanone selectivity for Pd/C catalyst and cyclohexanol selectivity for Pt/C catalyst.

eral reactor decrease as compared with the phenol EHP reactor. This relates to less adhesion of the Pd/C catalyst on GDL as observed in the experiments.

The data in this work indicate that two hydrogen-related reactions could be successfully performed simultaneously in one EHP reactor. The performance is almost as excellent as that in the individual EHP reactors. Therefore, costs for hydrogen production, storage and transportation, as well as reactor equipment could be saved to a large extent. Moreover, the bilateral EHP reactor provides a solution to the problem of hydrogen permeation across PEMs, which decreases the amount of catalyst active sites.

However, there is still a challenge for the bilateral EHP reactor proposed in this work. As shown in Fig. 9(a), the applied potential is much higher in the bilateral reactor as compared with the individual EHP reactors. In the individual

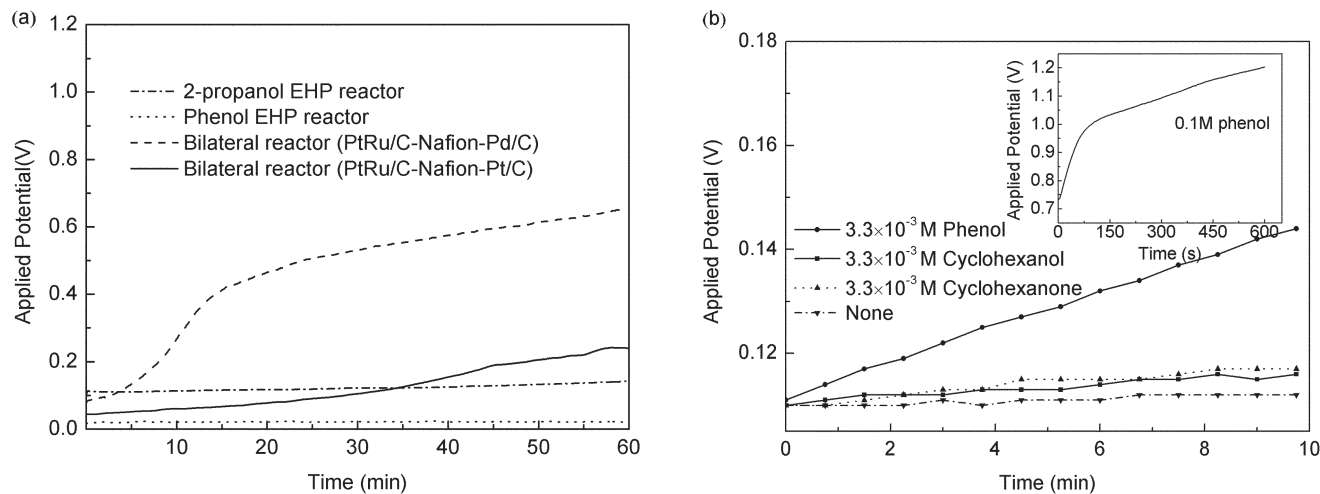


Fig. 9 (a) Applied potential of the 2-propanol dehydrogenation EHP reactor, phenol hydrogenation EHP reactor and bilateral EHP reactor with PtRu–Pd/C and PtRu–Pt/C MEAs; (b) applied potential of the 2-propanol dehydrogenation EHP reactor as a function of reaction time with different additives (reaction conditions: (a) 18.9 mA cm⁻², 80 °C; anode: 10 ml min⁻¹ 2-propanol, 1 M 2-propanol, catalyst loading 4.0 mg cm⁻²; cathode: 10 ml min⁻¹ phenol, 0.1 M phenol, catalyst loading 0.5 mg cm⁻²; (b) 18.9 mA cm⁻², 80 °C; anode: 10 ml min⁻¹ 2-propanol with additives, 1 M 2-propanol, catalyst loading: 4.0 mg cm⁻² (10 ml min⁻¹ phenol, 0.1 M phenol for inserted figure b)).

EHP reactors, the applied potential of the anodic 2-propanol dehydrogenation EHP reactor and the cathodic phenol hydrogenation EHP reactor are as low as around 0.1 V and 0.02 V, respectively. For the bilateral EHP reactor, although the starting applied potential is in between that of the anode and cathode, it increases gradually to 0.6 V with the proceeding of the reaction. It is assumed that the elevated potential is caused by cross contamination of the reactants across the Nafion membrane. In order to confirm this assumption, quantitative (3.3×10^{-3} M) additives, including the reactant phenol and products cyclohexanone and cyclohexanol are added into 1 M 2-propanol, respectively. The obtained mixture is used as an anode feedstock in the 2-propanol dehydrogenation reactor to simulate the cross contamination. As shown in Fig. 9(b), cyclohexanone and cyclohexanol have little effect on the applied potential, while the applied potential increases gradually as phenol is present in the 2-propanol solution, especially with a higher concentration of 0.1 M (inset in Fig. 9(b)). *p*-Benzoquinone is detected in the dehydrogenation products, which means that phenol at the cathode permeates through the Nafion membrane and dehydrogenates to produce *p*-benzoquinone at the anode. It is reported in the literature that the potential of the phenol dehydrogenation reaction is around 1.3 V.^{47,48} Hence, permeation of organic reagents through proton exchange membranes is an important issue to be considered in bilateral EHP reactors. Investigation of permeation resistant membranes is ongoing in our group.

4. Conclusions

The 2-propanol dehydrogenation reaction and phenol hydrogenation reaction are successfully achieved in one EHP bilateral reactor. In the 2-propanol dehydrogenation reaction at the

anode, the applied potential is much lower on the Pt–Ru/C than on the Pt/C catalyst. By applying a pulse current operation and increasing the catalyst loading and temperature, extensive dehydrogenation of 2-propanol on the Pt–Ru/C catalyst could be reduced, thus maintaining a lower applied potential of around 0.2 V within a 3 h reaction. The available current density of 2-propanol dehydrogenation on the Pt–Ru/C catalyst is up to 38 mA cm⁻², which supplies abundant *in situ* adsorbed hydrogen atoms for the hydrogenation reaction at the cathode. For the cathode phenol hydrogenation reaction, Pd/C catalyst is an excellent catalyst to generate cyclohexanone (selectivity of around 85%) while Pt/C catalyst has high selectivity (95.4% at 38 mA cm⁻²) for cyclohexanol. Reaction conditions, such as temperature, current density and reaction time are also investigated in terms of their effects on dehydrogenation and hydrogenation behaviours in the EHP reactor. Under optimal conditions, a 2-propanol dehydrogenation and phenol hydrogenation bilateral EHP reactor is successfully run with a comparable hydrogenation rate, conversion, selectivity and current efficiency. The highest hydrogenation rate is 121.0 mmol h⁻¹ g⁻¹_{Pd} (calculated by total products as shown in Fig. 8), which is much higher than that of the conventional three-phase reactor and electro-chemical dynamic reactor. The feasibility of the bilateral EHP reactor provides a novel idea to integrate multiple reactors into one configuration, reducing the cost of hydrogen production, storage and transportation, as well as reactor equipment.

Acknowledgements

The authors thank the Program for National Science Fund for Distinguished Young Scholars of China (Grant 21125628), NSFC (Grant 21176044 and 21476044) and the Program for

Liaoning Excellent Talents in University (LR2014003) for financial support of this work.

Notes and references

- S. Chu and A. Majumdar, *Nature*, 2012, **488**, 294–303.
- S. De, B. Saha and R. Luque, *Bioresour. Technol.*, 2015, **178**, 108–118.
- D. W. Green and R. H. Perry, *Perry's Chemical Engineers' Handbook*, McGraw-Hill, New York, 8th edn, 2007.
- G. W. Huber, S. Iborra and A. Corma, *Chem. Rev.*, 2006, **106**, 4044–4098.
- X. Wu, G. He, L. Yu and X. Li, *ACS Sustainable Chem. Eng.*, 2013, **2**, 75–79.
- X. Wu, J. Benziger and G. He, *J. Power Sources*, 2012, **218**, 424–434.
- S. K. Green, G. A. Tompsett, H. J. Kim, W. B. Kim and G. W. Huber, *ChemSusChem*, 2012, **5**, 2410–2420.
- S. K. Green, J. Lee, H. J. Kim, G. A. Tompsett, W. B. Kim and G. W. Huber, *Green Chem.*, 2013, **15**, 1869–1879.
- A. Sáez, V. García-García, J. Solla-Gullón, A. Aldaz and V. Montiel, *Electrochim. Acta*, 2013, **91**, 69–74.
- L. Xin, Z. Zhang, J. Qi, D. J. Chadderton, Y. Qiu, K. M. Warsko and W. Li, *ChemSusChem*, 2013, **6**, 674–686.
- J. Benziger and J. Nehlsen, *Ind. Eng. Chem. Res.*, 2010, **49**, 11052–11060.
- W. Chen, G. He, F. Ge, W. Xiao, J. Benziger and X. Wu, *ChemSusChem*, 2015, **8**, 196.
- M. N. Uddin and W. W. Daud, *Energy Fuels*, 2014, **28**, 4300–4320.
- C. Acar and I. Dincer, *Int. J. Hydrogen Energy*, 2014, **39**, 1–12.
- J. N. Keuler, L. Lorenzen and S. Miachon, *Appl. Catal., A*, 2001, **218**, 171–180.
- S. Lambert, C. Cellier, F. Ferauche, E. M. Gaigneaux and B. Heinrichs, *Catal. Commun.*, 2007, **8**, 2032–2036.
- N. Kariya, A. Fukuoka and M. Ichikawa, *Phys. Chem. Chem. Phys.*, 2006, **8**, 1724–1730.
- P. Sun, G. Siddiqi, W. C. Vining, M. Chi and A. T. Bell, *J. Catal.*, 2011, **282**, 165–174.
- A. S. Arico, S. Srinivasan and V. Antonucci, *Fuel Cells*, 2001, **1**, 133–161.
- F. Bresciani, C. Rabissi, M. Zago, R. Marchesi and A. Casalegno, *J. Power Sources*, 2015, **273**, 680–687.
- A. H. Sirk, J. M. Hill, S. K. Kung and V. I. Birss, *J. Phys. Chem. B*, 2004, **108**, 689–695.
- H. J. Kim, J. Lee, S. K. Green, G. W. Huber and W. B. Kim, *ChemSusChem*, 2014, **7**, 1051–1056.
- A. de Lucas-Consuegra, A. B. Calcerrada, A. R. De La Osa and J. L. Valverde, *Fuel Process. Technol.*, 2014, **127**, 13–19.
- M. Li, Y. Hao, F. Cárdenas-Lizana, H. H. P. Yiu and M. A. Keane, *Top. Catal.*, 2015, **58**, 149–158.
- Q. Yang, Y. Chen, Z. U. Wang, Q. Xu and H. Jiang, *Chem. Commun.*, 2015, **51**, 10419.
- D. Gao, H. Yin, Y. Feng and A. Wang, *Can. J. Chem. Eng.*, 2015, **93**, 1107–1118.
- D. Gao, Y. Feng, H. Yin, A. Wang and T. Jiang, *Chem. Eng. J.*, 2013, **233**, 349–359.
- D. Gao, H. Yin, A. Wang, L. Shen and S. Liu, *J. Ind. Eng. Chem.*, 2015, **26**, 322–332.
- A. Javaid and C. S. Bildea, *Chem. Eng. Technol.*, 2014, **37**, 1515–1524.
- Z. E. Tapan, *Turk. J. Chem.*, 2009, **33**, 487–499.
- Z. Qi and A. Kaufman, *J. Power Sources*, 2002, **112**, 121–129.
- B. Habibi and E. Dadashpour, *Electrochim. Acta*, 2013, **88**, 157–164.
- A. Santasalo, T. Kallio and K. Kontturi, *Platin Met. Rev.*, 2009, **53**, 58–66.
- J. Wang, S. Wasmus and R. F. Savinell, *J. Electrochem. Soc.*, 1995, **142**, 4218–4224.
- A. Demirbas, *Fuel Process. Technol.*, 2007, **88**, 591–597.
- B. Güvenatam, O. Kurşun, E. H. J. Heeres, E. A. Pidko and E. J. M. Hensen, *Catal. Today*, 2014, **233**, 83–91.
- C. M. Cirtiu, H. O. Hassani, N. Bouchard, P. A. Rowntree and H. Ménard, *Langmuir*, 2006, **22**, 6414–6421.
- Kirk-Othmer Encyclopedia of Chemical Technology*, ed. M. Howe-Grant, Wiley, New York, 1991.
- H. Liu, T. Jiang, B. Han, S. Liang and Y. Zhou, *Science*, 2009, **326**, 1250–1252.
- J. Zhu, G. Tao, H. Liu, L. He, Q. Sun and H. Liu, *Green Chem.*, 2014, **16**, 2664–2669.
- C. L. Green and A. Kucernak, *J. Phys. Chem. B*, 2002, **106**, 1036–1047.
- C. Lee, M. Umeda and I. Uchida, *J. Power Sources*, 2006, **160**, 78–89.
- Y. Ando, M. Yamashita and Y. Saito, *Bull. Chem. Soc. Jpn.*, 2003, **76**, 2045–2049.
- M. Yamashita, T. Kawamura, M. Suzuki and Y. Saito, *Bull. Chem. Soc. Jpn.*, 1991, **64**, 272–278.
- Y. Xu and L. Han, *Int. J. Hydrogen Energy*, 2014, **39**, 7278–7290.
- Y. Wang, J. Yao, H. Li, D. Su and M. Antonietti, *J. Am. Chem. Soc.*, 2011, **133**, 2362–2365.
- Z. Wu and M. Zhou, *Environ. Sci. Technol.*, 2001, **35**, 2698–2703.
- Y. J. Feng and X. Y. Li, *Water Res.*, 2003, **37**, 2399–2407.